frontiers | Frontiers in Earth Science

ORIGINAL RESEARCH
published: 13 June 2022
doi: 10.3389/feart.2022.835937

Paleoenvironmental Changes Since the Late Pleistocene Revealed by Ostracodes Record in Changmu Co., Western Tibet

*Gao Song and Hailei Wang**

MNR Key Laboratory of Saline Lake Resources and Environments, Institute of Mineral Resources, Chinese Academy of Geological Sciences, Beijing, China

A 4.9-m profile (BG-1) in Changmu Co., western Tibet, provides a continuous climate record from the Late Pleistocene to mid-Holocene on the basis of ostracode assemblages and shell trace elements. The results show six distinct climate change zones from 23.4 to 4.9 ka BP based on U-Th dating. The climate remained extremely cold until 13 ka BP because of the influence of the Last Glacial Maximum, which was indicated by the rare ostracodes occurring in this period. After that, the temperature rose gradually and the paleolake (Changmu Co.) enlarged. The ostracode assemblage during this period had high abundance and diversity, although the dominance of cold-water species and low Mg/Ca ratios indicate that the climate was still cold. More runoff water from a relatively warm climate entering into the lake, suggested by the increased U/Ca and Mn/Ca, led to a high lake level of 13–10.5 ka BP; this trend was also verified by the decreasing Sr/Ca values. The climate changed from humid to drought between 10.5 and 7.9 ka BP, which was inferred from the decreased abundance of ostracodes; however, there was a short humid period from 9.5 to 9.2 ka BP suggested by increased U/Ca and Mn/Ca ratios. A gradual transition to a humid environment began at 7.9 ka BP and ended at 5.3 ka BP. After this period, an extremely arid climate occurred after rising temperature and increasing evaporation, indicated by sharply increased Mg/Ca and Sr/Ca ratios. Eventually, the Changmu Co. paleolake shrank and dried up at some time after 4.9 ka BP. The changes in paleoclimate in Changmu Co. since the Late Pleistocene corresponded well to changes that occurred in the Westerlies-dominated Central Asia, suggesting that the climate in this region was mainly controlled by Westerlies circulation.

Keywords: ostracodes, trace elements, paleoclimate, late Pleistocene, Western Tibet

OPEN ACCESS

Edited by:
Zhang Chengjun,
Lanzhou University, China

Reviewed by:
Zhibang Ma,
Institute of Geology and Geophysics (CAS), China
Zhongping Lai,
Shantou University, China

****Correspondence:***
Hailei Wang
wanghailei77@126.com

Specialty section:
This article was submitted to Quaternary Science, Geomorphology and Paleoenvironment, a section of the journal Frontiers in Earth Science

Received: *15 December 2021*
Accepted: *25 April 2022*
Published: *13 June 2022*

Citation:
Song G and Wang H (2022) Paleoenvironmental Changes Since the Late Pleistocene Revealed by Ostracodes Record in Changmu Co., Western Tibet. Front. Earth Sci. 10:835937. doi: 10.3389/feart.2022.835937

INTRODUCTION

Lake sediment is a useful material for paleoenvironmental and paleoclimatic studies because of its wide distribution and excellent continuity. Lake sediment also contains a variety of proxies, such as pollen, diatoms, ostracodes, clastics, and carbonate materials (Bradley 1998; William et al., 2001). A large amount of valuable paleoenvironmental data has been obtained from lake sediments in various parts of the world, and these data have been widely used for regional comparison and reconstruction of the paleoenvironment (Kim et al., 2015; Li et al., 2016; Lu et al., 2017). Ostracodes are aquatic

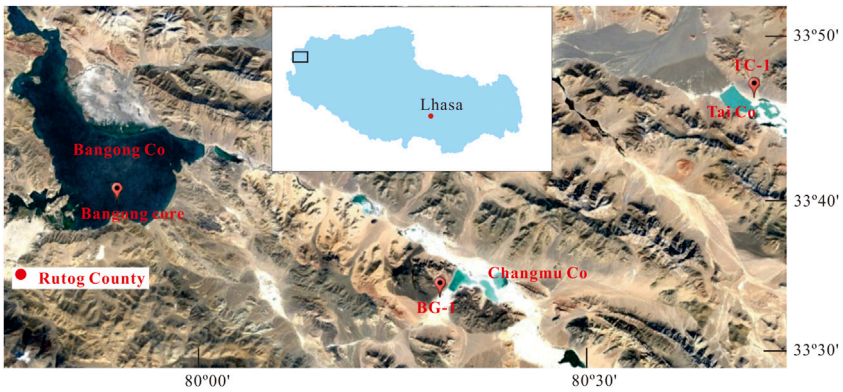

FIGURE 1 | Location of the research area in Tibetan Plateau and position of Bangong Co., Changmu Co., Tai Co., and BG-1 profile in western Tibetan Plateau.

bivalved crustaceans that live in most types of water bodies. They have a sensitive response to many environmental factors, including temperature, salinity, and lake water depth (Löffler, 1997; Curry, 1999; Yilmaz and Külköylüoglu, 2006; Song et al., 2015a), and they are important paleoenvironmental indicators in non-marine environments. Generally, different species of ostracodes prefer different environmental conditions and can flourish in these habitats (Yang et al., 2006). Ostracode shells, comprising low-Mg calcite, have also been used widely in paleoclimate studies (Chivas et al., 1983, Chivas et al., 1985, Chivas et al., 1986a, Chivas et al., 1986b; Holmes et al., 1995; Cronin et al., 2000; Schwalb, 2003; Decrouy et al., 2012; Schwalb et al., 2013). Trace element ratios in ostracode shells can be used as proxies for paleoclimate in lacustrine environments. The Mg/Ca molar ratio normally has a positive correlation with salinity and temperature of host water, while the Sr/Ca ratio is only positively related to the salinity of water (Holmes et al., 1999). The U/Ca ratio has been examined to infer past oxygen levels in the bottom water of the lake (Ricketts et al., 2001), with decreasing U/Ca value indicating lower oxygen availability (Yang et al., 2014). Mn can serve as a sensitive proxy for water level fluctuations in arid regions, and a long-term decrease in the input of Mn reflects a long-term climate drying (Yang et al., 2013).

A 12.4 m sediment core in the Lake Bangong basin, approximately 45 km to the west of Changmu Co., recorded environmental changes during the Holocene from 9.9 ka BP based on the radiocarbon ages (Fan et al., 1996; Fontes et al., 1996; Gasse et al., 1996; Van Campo et al., 1996). Climate changes and local hydrological factors may have induced extremely large changes in environmental conditions, which were revealed from the mineralogy, $\delta^{13}C$, and $\delta^{18}O$ contents of authigenic carbonates. The regional climatic change was the major driving factor for ecological and hydrobiological changes in the lakes of western Tibet, as indicated by these biogenic remains. However, these studies do not mention the cause of climate change in western Tibet, which is a critical question and requires more study of paleoclimate records. The characteristics of paleoclimate evolution in Changmu Co. were almost unknown before, but such information is required to discuss the controlling factors of climate change in western Tibet. Here, we present the records of ostracode assemblages and trace elements in two species (*Limnocythere dubiosa* and *Leucocythere subsculpta*) in a profile from Changmu Co. (**Figure 1**) to characterize the high-resolution climatic changes in western Tibet since the Late Pleistocene. We also compare these changes with the paleoclimate records from other lakes in arid Central Asia to discuss the controlling factors of climatic evolution.

GEOLOGICAL SETTING AND CLIMATE

The BG-1 profile (33°27′48.53″N, 80°16′44.62″E, 4,313 m) is on the bank of Changmu Co. (**Figure 1**). Lake Changmu Co. is located approximately 50 km east of Rutog County in western Tibet. The catchment geology is characterized by light-colored gravel, gravel-silty soil, silty clay, and calcareous clay of the Pleistocene and Holocene (Liu et al., 2013). The areas are surrounded by two mountain ranges, the Karakorum Mountain to the north and the Gangdise Mountain to the south. The two mountain chains are glacier-developing regions that can provide ice meltwater to Changmu Co.

The research area is located in an extremely arid and cold region. The mean annual precipitation is 87 mm according to NASDE monitoring data from 2010 to 2014 (Hou et al., 2002), which is about 1/30 of potential evapotranspiration. The mean annual air temperature is about 2°C.

MATERIALS AND METHODS

Profile BG-1 in Changmu Co. is about 490 cm thick. The upper 284-cm sediments were sampled at 4-cm intervals in the field for ostracode fossils, while it was sub-sampled at 5–6 cm intervals from 284 to 490 cm. Eight dating samples

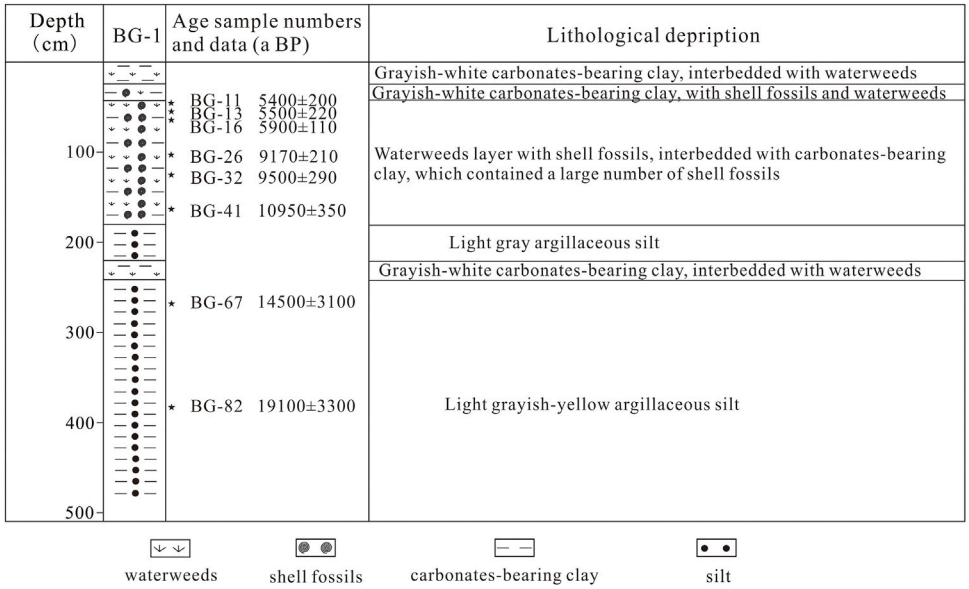

FIGURE 2 | Lithology characterization of BG-1 in Changmu Co. and eight U-series sample horizons in the profile with dating results.

collected at different horizons in the upper 4 m are shown in **Figure 2**.

^{230}Th/^{234}U Age Estimate in Carbonates and Experimental Procedures

U-series disequilibrium dating is based on the accumulation of ^{230}Th as a result of the incorporation of ^{238}U and ^{234}U into the $CaCO_3$ lattice at the time of formation. ^{230}Th is a daughter product of ^{234}U with a half-life of 75.2 ka. Because uranium solubility in natural water allows its precipitation with calcite, while thorium is quickly absorbed or precipitated as insoluble hydrolyzates when brought into solution, assuming that the initial amount of ^{230}Th and ^{232}Th incorporated into $CaCO_3$ is zero, most or all of the ^{230}Th measured in carbonates will have been derived from the decay of ^{234}U (Ma et al., 2012). The age of carbonates can be determined from the extent of disequilibria between ^{230}Th and ^{234}U and between ^{234}U and ^{238}U by the following equation (Kaufman and Broecker, 1965).

Eight samples, including five shell samples and three carbonate-bearing clay samples, were submitted to the Uranium Chronology Laboratory of the Institute of Geology and Geophysics, Chinese Academy of Sciences for U-series dating. The five shell samples and one carbonate-bearing clay sample (BG-41) had high amounts of carbonate, providing confidence that the U-series technique should be suitable for dating these samples. The samples of BG-67 and BG-82 contained much detritus, and we corrected the detrital ^{230}Th of them with the leachate–leachate (L/L) scheme (Schwarcz and Latham, 1989), which could be applied to impure carbonates and had yield-reliable age results in some cases (Peng et al., 2014). In order to establish a chronology, the Iso/Ex program (Ludwig and Titterington, 1994) was used to determine ^{232}Th-free (^{230}Th/^{238}U) and (^{234}U/^{238}U) compositions by Osmond type-II regression techniques in an X-Y-Z plot (Wang et al., 2021). The reliability of a derived isochron age can be established statistically using the probability of fit and the mean sum of weighted deviations (MSWD) (Ludwig and Titterington, 1994). In cases where an isochron can be reliably fitted to the data set (probability of fit≈1, MSWD≤1), it can be assumed that the uncertainties associated with the age are a function of the analytical uncertainties (Candy et al., 2005, Alcaraz-Pelegrina and Martínez-Aguirre, 2007; Ma et al., 2010b).

About 8–10 g of the subsamples were weighed and baked in an oven at 800°C for 2 h after samples were crushed and homogenized and then dissolved in 2 M HNO_3 (samples of BG-67 and BG-82 were dissolved with different nitric acid concentrations). As carrier and yield tracer, about 10 mg of Fe^{3+} and ^{228}Th-^{232}U spike was added to the sample solutions. Concentrated NH_4OH was then added to the solution to allow U and Th to co-precipitate with Fe. Briefly, the solution was centrifuged to separate the precipitate, subsequently dissolved in 8 M HCl, and loaded onto an 8-M HCl-conditioned anion exchange column (BIORAD AG1×8, 100–200 meshes, 10 × 1 cm). Thorium passed through the column, while U and Fe were retained by the resin. Iron was washed off the column with a solution of 8 M NH_4NO_3-0.1 M HNO_3. After removing the residual NH_4NO_3 with about 2 ml of 8 M HCl, U was eluted with 0.1 M HNO_3. The Th aliquot was evaporated to dryness and dissolved in concentrated HNO_3 to yield a 7 M HNO_3 solution that was then loaded onto the same anion column, being converted to the NO_3-form. Th was eluted off the column with 8 M HCl. The purified U and Th fractions were evaporated to dryness and taken up with 0.1 M HNO_3.

Th and U were then extracted with an 0.4-M TTA-benzene mixture at pH of 1–1.5 and 3–3.5 and evaporated onto stainless steel planchets heated on a hot plate. The planchets were burned to decompose the organic compounds in the extracted solution before final instrumental measurements. The recovery of this procedure is 85% for Th and 50% for U.

Alpha-spectra of U and Th isotopes were determined using an Octête plus alpha spectrometer, with a vacuum of 20 mT and an energy resolution (FWHM) of about 25 keV at 5.15 MeV. The measured alpha spectra of U and Th isotopes were corrected by variable factors (Ma et al., 2010a).

Ostracode Fossils Analysis and ICP-MS

Fifty grams of each sediment sample was soaked in deionized water for approximately 3 days and then sieved with a 200-mesh sieve. The sieved materials were dried at room temperature for the selection of ostracodes. We identified these ostracode species on the basis of "Chinese ostracode fossils (volume I and II)" (Hou et al., 2002; 2007). Two species of ostracodes, *Limnocythere dubiosa* and *Leucocythere subsculpta*, were selected and cleaned using a paintbrush with deionized water under the microscope for trace elements analysis in this study. All picked adult valves were generally well-preserved and hyaline. No dissolution evidence or clearly visible coating was observed on them. Totally, 38 valves for *L. dubiosa* and 43 valves for *L. subsculpta* were obtained from different depths of the BG-1 profile. After cleaning, the valves were dried and then fixed on glass slides using epoxy for ICP-MS analysis.

In situ trace element analysis for single valves was performed using an X-Series ICP-MS (Thermo Fisher Scientific, Germany) coupled with a J-100 343-nm Yb: Fiber femto-second laser ablation system (Applied Spectra, United States) housed at the National Research Center for Geoanalysis, Chinese Academy of Geological Sciences (CAGS), Beijing, China. Helium gas carrying the ablated sample aerosol from the chamber is mixed with argon make-up gas and nitrogen as an additional diatomic gas to enhance sensitivity. A baffled-type smoothing device was used in front of the ICP-MS to reduce fluctuation effects induced by laser-ablation pulsed and improve the quality of the data (Tunheng and Hirata., 2004). The ostracode valve samples were ablated for 50 s at a repetition rate of 8 Hz, at 10 J/cm^2, and ablation pits were ~50 μm in diameter. The calibration was performed externally using two NIST SRM 610 and one NIST SRM 612 for every 10 samples, with Ca as the internal standard to correct for instrument drift. Data reduction was carried out with the commercial software ICPMSDataCal 10.8 (Liu et al., 2008). Repeated analyses of the standards SRM 610 and SRM 612 indicate that both precision and accuracy are better than 10% for most analyzed elements (Li et al., 2018). Yang et al. (2014) suggested that the trace element ratios obtained by the spot analysis for the ostracode shells of the same taxa from the same depth in Tibet agreed well with that of the line-scan analysis and also reflected the hydrologic and hydrochemical

TABLE 1 | U-Th isotope data from the BG-1 profile in western Tibet.

Sample	Depth (cm)	Materials	^{238}U (ppm)	^{234}U (ppm)	^{230}Th (ppm)	^{232}Th (ppm)	^{234}U/^{238}U	^{230}Th/^{232}Th	^{230}Th/^{234}U	Age (a BP) (uncorrected)	Age* (a BP) (corrected)
BG-11	44	shells	3.477 ± 0.114	72.533 ± 2.002	3.682 ± 0.119	0.179 ± 0.015	1.688 ± 0.058	20.551 ± 1.786	0.051 ± 0.002	5,700 ± 220	5,400 ± 200
BG-13	52	shells	8.908 ± 0.406	186.618 ± 7.421	9.671 ± 0.280	0.632 ± 0.046	1.695 ± 0.074	15.302 ± 1.196	0.052 ± 0.002	5,800 ± 230	5,500 ± 220
BG-16	64	shells	13.477 ± 0.233	269.875 ± 4.333	15.417 ± 0.293	1.475 ± 0.073	1.620 ± 0.022	10.454 ± 0.543	0.571 ± 0.001	6,370 ± 110	5,900 ± 110
BG-26	104	shells	5.566 ± 0.085	117.686 ± 1.469	9.767 ± 0.190	0.257 ± 0.018	1.711 ± 0.029	38.066 ± 2.821	0.083 ± 0.002	9,360 ± 210	9,170 ± 210
BG-32	128	shells	5.758 ± 0.111	118.773 ± 1.898	10.233 ± 0.273	0.225 ± 0.013	1.669 ± 0.036	45.453 ± 2.901	0.086 ± 0.003	9,800 ± 290	9,500 ± 290
BG-41	164	carbonate	2.906 ± 0.085	60.835 ± 1.521	6.139 ± 0.174	0.357 ± 0.025	1.694 ± 0.051	17.220 ± 1.293	0.101 ± 0.003	11,400 ± 390	10,950 ± 350

**Corrected. ^{230}Th ages assuming that (i) initial. ^{230}Th/^{232}Th activity ratios are 0.764 and those are the values for a material at secular equilibrium, with the upper continental crust. ^{232}Th/^{238}U mass ratio of 4.1 (Wedepohl, 1995); (ii) initial non-detrital. ^{230}Th is equal to 0.*

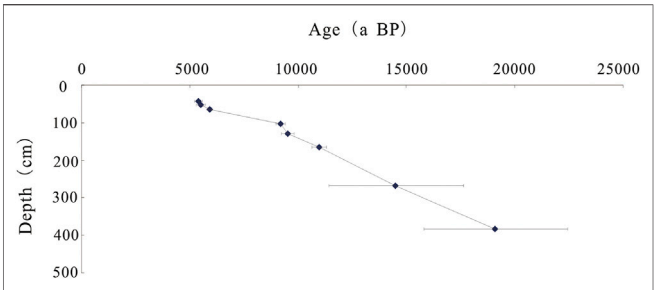

FIGURE 3 | U-series chronological results of profile BG-1.

changes effectively in the lake system, so we carried out two craters for each sample, and we assumed that the mean value was representative of the composition of the whole specimen.

RESULT

Chronology

The results of the radiochemical analyses on each of the samples are listed in **Tables 1**, **2**. Activity ratios of $^{234}U/^{238}U$ of six samples in **Table 1** range from 1.620 to 1.711, and the similar uranium isotopic ratios in the whole sequence indicate that the source of lake water is uniform in the Changmu Co. area and the sedimentary environment is relatively stable. In **Table 2**, the POF and MSWD of BG-67 and BG-82 are 0.012 and 2.5 and 0.076 and 1.8, respectively, meaning the dispersion degree of each subsample on the isochron is large, which may reduce the reliability of the dating. However, the two ages fall in the whole age profile sequence, which has a good corresponding relationship with the stratigraphic sequence. Therefore, the two age data can be acceptable geologically.

Sediments in the upper 4 m of profile BG-1 recorded environmental evolution history in this area during 19.1–5.4 ka BP. Comparing the ages with corresponding positions in the profile, all ages were in stratigraphic order within the analytical errors, which allowed the establishment of a reliable chronology (**Figures 2**, **3**). We plotted the age of 4.9 ka BP on the top of the BG-1 profile and 23.4 ka BP at the bottom by extrapolation due to the similar lithology. Most sedimentation rates varied from 0.12 mm/a to 0.29 mm/a, except 0.8 mm/a during 5,500 to 5,400 a BP and 0.73 mm/a during 9,500–9,170 a BP. The huge differences in sedimentation rate were highly related to the variations in lithology. From 5,500 to 5,400 a BP, the lithology was dominated by waterweeds, while during 9,170–9,500 a BP, shell fossils dominated. The rapid growth of waterweeds and shells resulted in a higher sedimentation rate.

Ostracode Assemblages

A total of 106 samples were analyzed for ostracode fossils, and 62 samples contained ostracode shells. The largest abundance appeared at 12.2 ka BP with about 890 shells/g. The shells were especially common in the depth of 224–152 cm (13–10.5 ka BP) but almost absent at the phases of 180–168 cm (11.5–11.1 ka BP) and 104–88 cm (9.2–7.9 ka BP) in the BG-1 profile (**Figure 5**). Totally 13 species, belonging to eight genera were identified (**Figure 4**), that is, *Limnocythere binoda*, *L. dubiosa*, *Leucocythere subsculpta*, *L. parasculpta*, *Candona houae*, *C. neglecta*, *C. candida*, *Candoniella lacteal*, *Ilyocypris gibba*, *I. bradyi*, *Limnocytherellina trispinosa*, *Heterocypris salinus*, and *Eucypris mareotica*, in which, *L. dubiosa* and *L. subsculpta* were the dominant species.

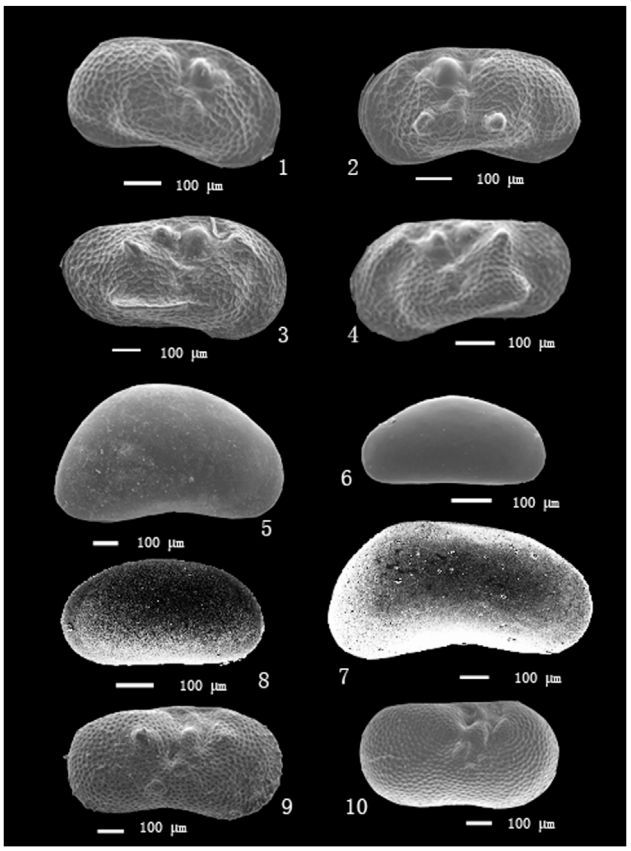

FIGURE 4 | Dominant species of ostracodes from the BG-1 profile in Changmu Co. area. 1. *Limnocythere dubiosa*, Rv; 2. *Limnocythere binoda*, Lv; 3. *Leucocythere subsculpta*, Rv; 4. *Leucocythere parasculpta*, Lv; 5. *Candona candida*, Rv; 6. *Candona houae*, Rv; 7. *Candona neglecta*, Rv; 8. *Candoniella lacteal*, Lv; 9. *Ilyocypris gibba*, Rv; and 10. *Ilyocypris bradyi*, Rv.

Trace Element Chemistry of Ostracode Shells

Figure 6 shows the molar ratios of Mg/Ca, Sr/Ca, U/Ca, and Mn/Ca in the shells of *Limnocythere dubiosa* and *Leucocythere subsculpta*. Mg/Ca shows comparable values between the two species. Higher U/Ca and Mn/Ca are observed in *L. dubiosa*, while it is reverse in Sr/Ca, which should be attributed to the different habitats between *L. subsculpta* and *L. dubiosa*. *Leucocythere* inhabits the upper few centimeters of the bottom sediments, while *Limnocythere* lives mainly on the

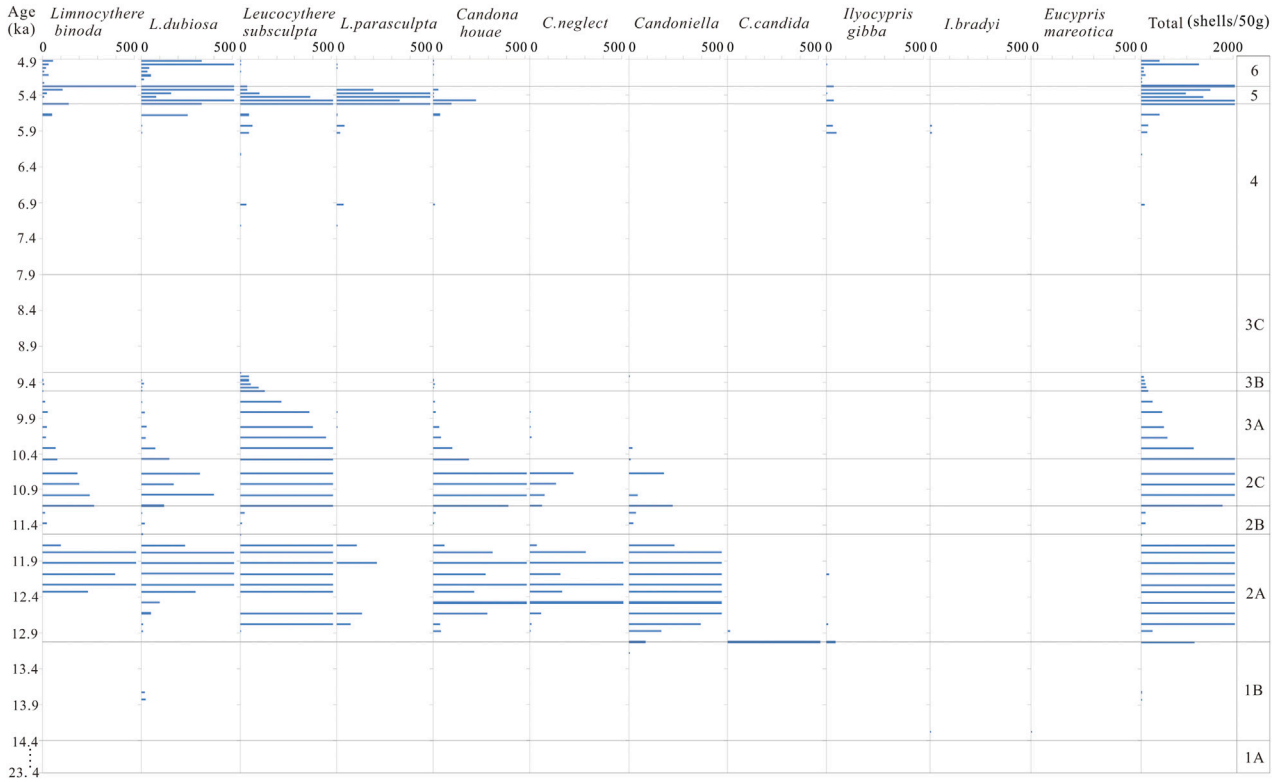

FIGURE 5 | Ostracode abundance diagram (shells per 50 g sediment) of profile BG-1.

bottom with abundant plant debris because it cannot swim (Meisch, 2000). The climate-driven salinity variations in the arid regions of the Tibetan Plateau during the Holocene period were mainly due to the precipitation/evaporation (P/E) balance (Dorberschütz et al., 2013; Kasper et al., 2013), so compared to *Limnocythere*, *Leucocythere* should be more sensitive to the salinity fluctuation of lake water but relatively insensitive to the change of water depth. Generally, Mg/Ca and Sr/Ca exhibit similar fluctuations, with relatively low and stable values from 13 to 7.9 ka BP and higher values from 7.9 to 4.9 ka BP. Both U/Ca and Mn/Ca have the tendency of increasing from 13 to 10.5 ka BPand then decrease gradually until 9.2 ka BP. The other increases of U/Ca and Mn/Ca appear during 7.9–5.5 ka BP, and after 5.5 ka BP, both of them decrease again.

DISCUSSION

Paleoclimate Change Inferred From Ostracodes in Changmu Co. Since 23.4 ka BP

Based on the variations of ostracode abundance (**Figure 5**) and the trace element ratios (**Figure 6**), we discussed the possible climate changes in Changmu Co. area since the Late Pleistocene in the following paragraphs.

From 23.4 to 14.4 ka BP (zone 1A), there were almost no ostracodes present, likely because of the extremely cold climate induced by the Last Glacial Maximum (LGM). *Ilyocypris bradyi*, *Limnocypris dubiosa*, and *Eucypris mareotica* began to appear in zone 1B (14.4–13 ka BP), indicating that the temperature rose slightly compared with zone 1A. From the investigation of living ostracodes on the Qinghai–Tibetan Plateau, Song et al.(2015a); Song et al.(2015b) concluded that *I. bradyi* was widely distributed in fresh-brackish water bodies (salinity <5‰). This species preferred slow-running water and was found commonly in streams, ponds, and springs (Meisch, 2000; Yang et al., 2006; Liu et al., 2007). *L. dubiosa* can live in fresh, brackish, and saline water bodies but flourished in fresh-brackish waters (salinity<5‰) and polyhaline–euhaline waters (18‰–40‰), and they were the most widely distributed ostracodes on the plateau. *E. mareotica* was the dominant species in polyhaline waters (18‰–30‰) on the Qinghai–Tibetan Plateau; this species was eurythermal and could tolerate low temperatures. Therefore, the appearance of these three species from 14.4 to 13 ka BP indicates that there was a small amount of runoff water entering into the paleolake Changmu Co. because of the temperature increase after the LGM; however, the lake water was still saline, as indicated by the continuous appearance of the saline water species *E. mareotica* and *L. dubiosa*.

In zone 2 (13–10.5 ka BP), most of the ostracodes (i.e., *Limnocythere binoda*, *L. dubiosa*, *Leucocythere subsculpta*, *Candona houae*, *C. neglecta*, and *Candoniella lacteal*) were present at a maximum abundance, except in zone 2B

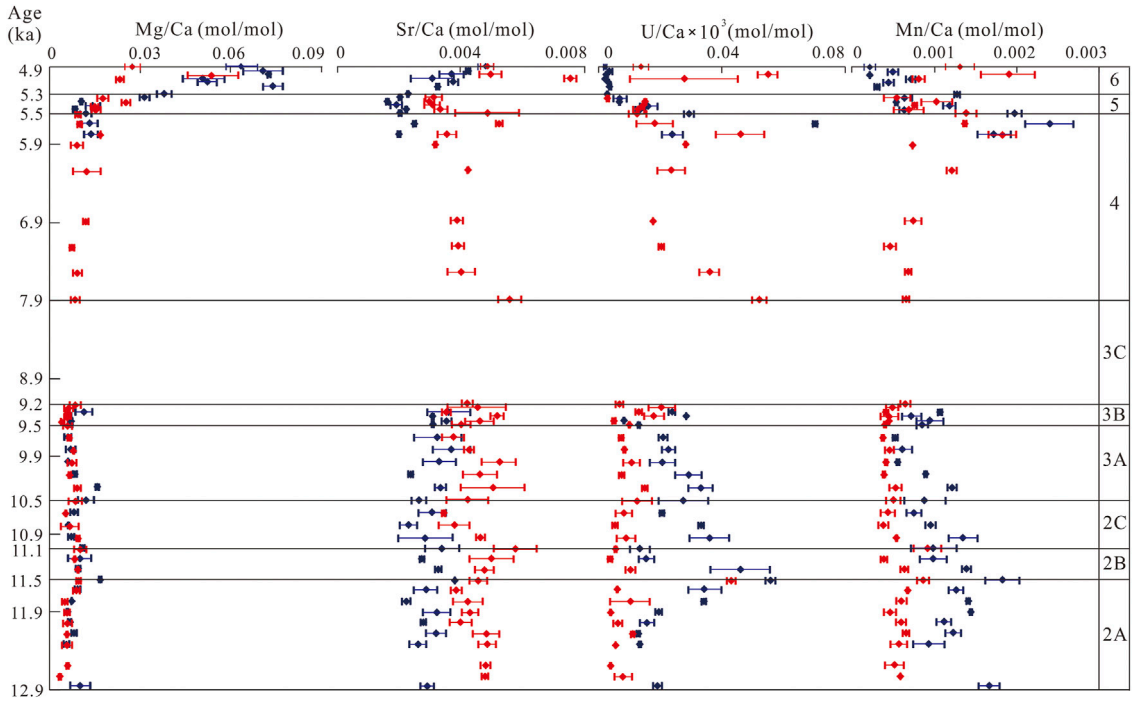

FIGURE 6 | Curves showing ratios of Mg/Ca, Sr/Ca, Mn/Ca, and U/Ca from ostracode shells; red spots represent molar ratios of *Leucocythere subsculpta* and blue spots represent molar ratios of *Limnocythere dubiosa*.

(11.5–11.1 ka BP). *Candona* preferred fresh and cold water, with a temperature of <10°C (IEDQPA and NJGP, 1988). *C. neglecta* was mainly found in freshwater (salinity<0.5‰), with a temperature range of 5–8°C (Lu et al., 2019), and *C. candida* was very abundant in Pleistocene cold-climate deposits. *Candoniella* also preferred fresh-brackish water (Yang et al., 2006; Song et al., 2015a). Most species of *Leucocythere* were euryhaline; they were distributed widely in sediments from the Pliocene to Quaternary (Huang et al., 1985) and preferred cold environments (Liu et al., 2007). The flourishing of these species suggested that the water level of paleolake Changmu Co. increased, but the temperature was still low; this was inferred from the low Mg/Ca and Sr/Ca ratios but high Mn/Ca and U/Ca ratios in the shells of both species (**Figure 6**). As shown in **Figures 4**, **5**, zone 2 could be divided into three sub-zones.

From 13 to 11.5 ka BP (zone 2A), ostracodes preferring cold and fresh-brackish waters, such as *Candona neglecta*, *C. houae*, *Candoniella lacteal*, and *Leucocythere subsculpta*, were the dominant species, which indicated cold and humid environment. The slightly increasing values of Mg/Ca during this period suggested that the temperature increased a little compared with zone 1 after the LGM, which induced more and more glacier meltwater into Changmu Co. The inflow of fresh melt-water not only enhanced the vertical mixing of the water column and increased the oxygen content of the lake bottom but also reduced the salinity of lake water, which was supported by the rapid increase of U/Ca and Mn/Ca and slight reduction of Sr/Ca in ostracode shells.

However, the warming trend was interrupted by an extremely detrimental condition that occurred in zone 2B (11.5–11.1 ka BP), characterized by a sharp decrease in ostracode abundance (**Figure 5**), which is attributed to the Younger Dryas (YD) event. The YD event had a global effect and was characterized by extremely cold weather (Jessen, 1938; Shen et al., 1996; deMenocal and Joseph, 2000; Genty et al., 2006; Liu et al., 2013; Cheddadi and Khater, 2016). In Bangong Co., no ostracode fossils were observed from 11.5 to 10 ka BP, which is likely attributable to the YD event (Li et al., 1994; Shen et al., 1996). In Changmu Co., the Mg/Ca ratios were steady and low in both species in zone 2B, implying the continuous low temperature. Mg/Ca in ostracode calcite depends on water salinity and temperature, but this dependence may be easily eclipsed by small Mg/Ca changes in the ambient water (De Deckker et al., 1999). Minor changes in the Mg/Ca ratio in zone 2B may be attributed to the changes in the Mg/Ca ratio of the host water during this extremely cold climate. The significant reduction in the U/Ca values may indicate less meltwater flowing into Changmu Co. and weak mixing that reduced the water level, demonstrated by the decreased Mn/Ca values. Compared with zone 2A, the average Sr/Ca ratio increased from 0.0029 to 0.0031 and from 0.0045 to 0.0052 in *Limnocypris dubiosa* and *Leucocythere subsculpta*, respectively, indicating that the salinity of the lake water increased. A possible explanation for this condition is that colder conditions during the YD event reduced the input of meltwater into Changmu Co., resulting in decreased oxygen availability in the host water and reduced water level. In these circumstances, the salinity of the lake water increased because of the strong evaporation.

The end of the YD event marks the warm beginning of the Holocene (Ding et al., 2014). This period coincided with a warm climate between 11.1 and 10.5 ka BP (zone 2C), as

indicated by the restoration of the ostracode population. However, the dominance of certain species (i.e., *Candida*, *Candoniella*, and *Leucocythere*) suggested that the temperature was still low, which is also indicated by the low Mg/Ca ratios. During this period, the Sr/Ca ratios decreased, while the U/Ca ratios increased, implying a decrease in water salinity and an increase in oxygen availability in the host water induced by the inflow of fresh meltwater. The Mn/Ca ratios decreased slightly and may indicate that the water level dropped slightly because of the negative precipitation/evaporation balance.

In zone 3 (10.5–7.9 ka BP), the abundance of ostracode decreased gradually until extinction at about 9.2 ka BP, suggesting the aridity environment in this period. Zone 3 could be divided into three sub-zones as shown in **Figure 6**.

From 10.5 to 9.5 ka BP (zone 3A), decreased U/Ca and Mn/Ca indicated that there was reduced runoff into the lake and reduced lake level, while the increased Sr/Ca ratio implied that the salinity of lake water was increasing. These trends coincided well with those of the decreased ostracode abundance.

There was a short humid period between 9.5 and 9.2 ka BP (zone 3B), inferred by the increased U/Ca and Mn/Ca ratios and the decreased Sr/Ca ratio, but the abundance of ostracodes was still reduced. This may be attributed to the unsuitable environment occurring after the extreme drought climate.

Because there were no ostracodes observed from 9.2 to 7.9 ka BP (zone 3C), it is difficult to interpret the paleoclimate changes during this period. Zheng et al. (2012) reported a gradual drought from 10.3 ka BP to 7.9 ka BP in Tai Co., approximately 45 km northeast of Changmu Co., on the basis of ostracodes and charophytes. In the Bangong Co. area from 8.6 to 7.5 ka BP, there was significant lake regression, indicated by increasing littoral and saline diatom species (Gasse et al., 1996). Therefore, we inferred that the disappearance of ostracodes in zone 3C indicated a continuous arid environment.

The fluctuations of trace elements clearly indicate the changing paleoclimate between 7.9 and 5.5 ka BP (zone 4), although there was a low abundance of ostracodes. During this period, the distinctly increased Mg/Ca ratio suggested that the temperature was rising after 7.9 ka BP, leading to more meltwater flowing into the paleolake of Changmu Co. This increased the water level and decreased the water salinity, as inferred from the increased Mn/Ca and decreased Sr/Ca ratios. Lower oxygen levels in the bottom waters were indicated by the decreased U/Ca between 7.9 and 6.9 ka BP, which was possibly due to the water plants being mainly present in the stratum. Increased decomposition of organic matter consumes more oxygen in the host water, resulting in more reducing conditions at the lake floor (Yang et al., 2014). From 6.9 to 5.5 ka BP, the increasing U/Ca values implied strong mixing and increased oxygen availability at the lake bottom, along with more meltwater flowing into the lake.

An optimum period occurred from 5.5 to 5.3 ka BP (zone 5), although the lake level dropped slightly (inferred from decreased Mn/Ca and U/Ca). A large number of *Limnocythere* and *Leucocythere* and a small number of *Candona* re-appeared, suggesting a humid environment. The climate became warmer,

TABLE 2 | Isochron age of profile BG-1.

Sample	Depth (cm)	Materials	^{238}U (ppm)	^{234}U (ppm)	^{230}Th (ppm)	^{232}Th (ppm)	$^{234}U/^{238}U$	$^{230}Th/^{238}U$	$^{232}Th/^{238}U$	MSWD	POF	Osmond Type-II regression line age (a BP)
BG-67 (1)	268	carbonate	1.621 ± 0.040	30.218 ± 0.628	11.153 ± 0.303	13.354 ± 0.330	1.509 ± 0.045	0.559 ± 0.020	0.667 ± 0.023	2.5	0.012	14500 ± 3100
(2)			1.945 ± 0.049	35.616 ± 0.763	14.321 ± 0.328	17.326 ± 0.358	1.482 ± 0.045	0.585 ± 0.020	0.721 ± 0.024			
(3)			2.124 ± 0.049	39.212 ± 0.760	25.554 ± 0.584	30.078 ± 0.632	1.494 ± 0.042	0.973 ± 0.032	1.146 ± 0.036			
(4)			2.058 ± 0.059	38.390 ± 0.915	24.489 ± 0.582	37.971 ± 0.741	1.509 ± 0.052	0.963 ± 0.036	1.493 ± 0.051			
(5)			1.264 ± 0.038	27.218 ± 0.065	2.437 ± 0.128	0.478 ± 0.044	1.391 ± 0.074	1.332 ± 0.073	1.773 ± 0.092			
(6)			5.566 ± 0.085	117.686 ± 1.469	9.767 ± 0.190	0.257 ± 0.018	1.348 ± 0.069	1.498 ± 0.061	2.467 ± 0.094			
BG-82 (1)	383	carbonate	0.564 ± 0.016	9.739 ± 0.230	4.237 ± 0.144	4.697 ± 0.150	1.398 ± 0.049	0.608 ± 0.027	0.674 ± 0.027	1.8	0.076	19100 ± 3300
(2)			1.363 ± 0.043	23.773 ± 0.637	12.375 ± 0.420	14.748 ± 0.456	1.412 ± 0.054	0.735 ± 0.034	0.876 ± 1.038			
(3)			1.307 ± 0.045	22.661 ± 0.673	14.121 ± 0.541	16.024 ± 0.567	1.403 ± 0.060	0.875 ± 0.039	0.992 ± 0.049			
(4)			2.059 ± 0.065	35.600 ± 0.979	23.713 ± 0.753	34.623 ± 0.923	1.399 ± 0.055	0.932 ± 0.042	1.360 ± 0.056			
(5)			1.672 ± 0.047	28.752 ± 0.709	23.218 ± 0.692	32.513 ± 0.833	1.391 ± 0.048	1.124 ± 0.046	1.573 ± 0.060			
(6)			2.781 ± 0.119	47.800 ± 1.768	45.775 ± 1.537	60.928 ± 1.781	1.390 ± 0.075	1.332 ± 0.073	1.773 ± 0.092			

(1)–(5), respectively, means dissolving the sample with different concentrations of HNO_3; (6) is the fully soluble sample.

as indicated by the gradually increasing Mg/Ca ratio, but the water salinity remained low, as indicated by low Sr/Ca; this result was compatible with the last bloom of freshwater species during 5.5–5.2 ka BP in Bangong Co. (Fan et al., 1996).

From 5.3 to 4.9 ka BP (zone 6), the temperature continued to rise, resulting in increased evaporation and an extremely dry climate, as indicated by the sharply increased Mg/Ca and Sr/Ca ratios. The U/Ca and Mn/Ca ratios continued to decrease, implying very little runoff into Changmu Co. The abundance and diversity of ostracodes decreased significantly during this period, and the low number of *Limnocythere* also indicated very high water salinity in an arid climate. After this period, the drought intensified further, and Changmu Co. shrank rapidly and eventually dried up at some time after 4.9 ka BP. The specific time when the paleolake Changmu Co. dried up was not determined, but it likely happened after 4.9 ka BP because the top of the profile BG-1 was 4.9 ka BP. When the paleolake water retreated from the area, the upper strata were eroded and not recorded in the profile.

The extremely dry climate after 5.3 ka BP, and especially after 4.9 ka BP, was also reflected in other records from lakes near Changmu Co. Profile TC-1 in Tai Co. (**Figure 1**) had a top age of 4.5 ka BP, implying a severely arid environment after 4.5 ka BP (Zheng et al., 2012). Sumxi Co. and Longmu Co. are two closed lakes situated approximately 120 km north of Changmu Co.; these lakes recorded decreases in the A/C ratio and heavy isotope contents at about 4.7–4.4 ka BP, also reflecting aridification (Gasse et al., 1991). In summary, all these records suggest that a large-scale drought event happened in the western Tibetan Plateau after 4.9 ka BP.

Comparison With Climate Records in Other Regions

It was very cold in Changmu Co. during the Late Pleistocene because of the LGM. Although the temperature rose slightly during the Early Holocene, as implied by the emergence of a large number of ostracodes, the dominance of the species *Candona*, *Candoniella*, and *Leucocythere* indicated that there was still a continuously cold environment. During this period, the paleolake expanded with meltwater supply, which is similar to Balikun Lake in the Westerlies-dominated region (Zhao et al., 2017) and Chibuzhang Co. in the north of Tibet (Dong et al., 2021). The alkenone records in Balikun Lake and the ostracode records in Chibuzhang Co. indicated that the rising temperature during the Late Pleistocene and Early Holocene led to more meltwater flowing into the lakes, rapidly increasing the water level.

Chen et al. (2008) concluded that the climate was arid during 11–8 ka BP, humid from 8 to 5 ka BP, and arid again after 5 ka BP, as determined by summarizing the sedimental records of 11 lakes in the Westerlies-dominated Central Asia. Alivernini et al. (2018) demonstrated that the Taro Co. areas, located in the south of Tibet, reached its highest level of the entire Holocene during 11.2–9.7 ka cal BP based on OSL dating and ostracod analysis. The ostracode assemblages and trace elements indicated that Changmu Co. was arid during 10.5–7.9 ka BP, humid during 7.9 to 5.3 ka BP, and arid again after 5.3 ka BP, which corresponded well to the paleoclimate changes in the Westerlies-dominated Central Asia and was a reverse of what was determined in Taro Co. areas. Zhao et al. (2017) determined that it was cold before 8 ka BP but increasingly warmer after 8 ka BP in Westerlies-dominated Central Asia, as inferred from the alkenone records in Balikun Lake. In Changmu Co., the constant low Mg/Ca ratios in ostracode shells also indicated a cold climate before 7.9 ka BP. After this period, the temperature increased gradually, as implied by the increased Mg/Ca ratios. Based on our data and previous studies, we infer that the paleoclimate change in Changmu Co. since the Late Pleistocene was mainly affected by Westerlies circulation.

CONCLUSION

A high-resolution ostracode record spanning from 23.4 to 4.9 ka BP was retrieved in Changmu Co., western Tibet. The climate remained cold until 7.9 ka BP and became especially warm after 5.5 ka BP. Changmu Co. enlarged sharply after the LGM and was interrupted by a shrink during 10.5–7.9 ka BP. At about 5.3 ka BP, and especially after 4.9 ka BP, a large-scale extreme drought event happened in the western Tibetan Plateau.

The changes in paleoclimate in Changmu Co. since the Late Pleistocene corresponded well to changes that occurred in the Westerlies-dominated Central Asia, indicating that the climate in this region was mainly controlled by Westerlies circulation.

DATA AVAILABILITY STATEMENT

The original contributions presented in the study are included in the article/Supplementary Material; further inquiries can be directed to the corresponding author.

AUTHOR CONTRIBUTIONS

GS handled the ostracode fossils of the samples and the experiments of trace elements and wrote this manuscript; HW collected the samples and designed the experiments.

FUNDING

This study was supported by the National Natural Science Foundation of China (No. U20A20148 and No. 41372179), the Fundamental Research Funds for Central Leveled Scientific Research Institutes (JYYWF20182701).

ACKNOWLEDGMENTS

We thank Professor Yang Fan from the Research Institute of Exploration and Development, Qinghai Oilfield Company for ostracode identification. This company was not involved in the study design, collection, analysis, interpretation of data, the writing of this article or the decision to submit it for publication.

REFERENCES

Alcaraz-Pelegrina, J. M., and Martínez-Aguirre, A. (2007). U/Th Dating of Carbonate Deposits from Constantina (Sevilla), Spain. *Appl. Radiat. Isotopes* 65, 798–804. doi:10.1016/j.apradiso.2007.01.006

Alivernini, M., Lai, Z., Frenzel, P., Fürstenberg, S., Wang, J., Guo, Y., et al. (2018). Late Quaternary Lake Level Changes of Taro Co and Neighbouring Lakes, Southwestern Tibetan Plateau, Based on OSL Dating and Ostracod Analysis. *Glob. Planet. Change* 166, 1–18. doi:10.1016/j.gloplacha.2018.03.016

Bradley, R. S. (1998). *Paleoclimatology-reconstructing Climate of the Quaternary*. USA: Academic Press, 613.

Candy, I., Black, S., and Sellwood, B. W (2005). U-Series Isochron Dating of Immature and Mature Calcretes as a Basis for Constructing Quaternary Landform Chronologies for the Sorbas Basin, Southeast Spain. *Quat. Res.* 64, 100–111. doi:10.1016/j.yqres.2005.05.002

Cheddadi, R., and Khater, C. (2016). Climate Change since the Last Glacial Period in Lebanon and the Persistence of Mediterranean Species. *Quat. Sci. Rev.* 150, 146–157. doi:10.1016/j.quascirev.2016.08.010

Chen, F., Yu, Z., Yang, M., Ito, E., Wang, S., Madsen, D. B., et al. (2008). Holocene Moisture Evolution in Arid Central Asia and its Out-of-phase Relationship with Asian Monsoon History. *Quat. Sci. Rev.* 27, 351–364. doi:10.1016/j.quascirev.2007.10.017

Chivas, A. R., De Deckker, P., and Shelley, J. M. G. (1986b). Magnesium and Strontium in Non-marine Ostracod Shells as Indicators of Palaeosalinity and Palaeotemperature. *Hydrobiologia* 143, 135–142. doi:10.1007/bf00026656

Chivas, A. R., De Deckker, P., and Shelley, J. M. G. (1986a). Magnesium Content of Non-marine Ostracod Shells: a New Palaeosalinometer and Palaeothermometer. *Palaeogeogr. Palaeoclimatol. Palaeoecol.* 54, 43–61. doi:10.1016/0031-0182(86)90117-3

Chivas, A. R., De Deckker, P., and Shelley, J. M. G. (1983). "Magnesium, Strontium and Barium Partitioning in Nonmarine Ostracod Shells and Their Use in Palaeoenvironmental Reconstructions-Aa Preliminary Study," in *Applications of Ostracoda*. Editor R. F. Maddocks (Houston, Texas: Geoscience Department, University of Houston), 238

Chivas, A. R., De Deckker, P., and Shelley, J. M. G. (1985). Strontium Content of Ostracods Indicates Lacustrine Palaeosalinity. *Nature* 316, 251–253. doi:10.1038/316251a0

Cronin, T. M., Dwyer, G. S., Baker, P. A., Rodriguez-Lazaro, J., and DeMartino, D. M. (2000). Orbital and Suborbital Variability in North Atlantic Bottom Water Temperature Obtained from Deep-Sea Ostracod Mg/Ca Ratios. *Palaeogeogr. Palaeoclimatol. Palaeoecol.* 162, 45–57. doi:10.1016/s0031-0182(00)00104-8

Curry, B. (1999). An Environmental Tolerance Index for Ostracodes as Indicators of Physical and Chemical Factors in Aquatic Habitats. *Palaeogeogr. Palaeoclimatol. Palaeoecol.* 148 (1), 51–63. doi:10.1016/s0031-0182(98)00175-8

De Deckker, P., Chivas, A. R., and Shelley, J. M. G. (1999). Uptake of Mg and Sr in the Euryhaline Ostracod *Cyprideis* Determined from *In Vitro* Experiments. *Palaeogeogr. Palaeoclimatol. Palaeoecol.* 148, 105–116. doi:10.1016/s0031-0182(98)00178-3

Decrouy, L., Vennemann, T. W., and Ariztegui, D. (2012). Mg/Ca and Sr/Ca of Ostracod Valves from Living Species of Lake Geneva. *Chem. Geol.* 314-317, 45–56. doi:10.1016/j.chemgeo.2012.04.007

deMenocal, P., Ortiz, J., Guilderson, T., and Sarnthein, M. (2000). Coherent High- and Low-Latitude Climate Variability during the Holocene Warm Period. *Science* 288 (5474), 2198–2202. doi:10.1126/science.288.5474.2198

Ding, X. D., Zheng, L. W., and Gao, S. J. (2014). A Review on the Young Dryas Event. *Adv. Earth Sci.* 29 (10), 1095. doi:10.11867/j.issn.1001-8166.2014.10.1095

Dong, N., Zhu, L. P., Chen, H., Ju, J. T., Peng, P., Wang, J. B., et al. (2021). Climate Changes of Past 13000 Years Based on Ostracod in Chibuzhang Co, Tibetan Plateau. *Quat. Sci.* 41 (2), 434. doi:10.11928/j.issn.1001-7410.2021.02.12

Dorberschütz, S., Frenzel, P., Haberzettl, T., Kasper, T., Wang, J., Zhu, L., et al. (2013). Monsoonal Forcing of Holocene Paleoenvironmental Change on the Central Tibetan Plateau Inferred Using a Sediment Record from Lake Nam Co (Xizang, China). *J. Paleolimnol.* 51, 253–266.

Fan, H., Gasse, F., Huc, A., Li, Y., Sifeddine, A., and Soulié-Märsche, I. (1996). Holocene Environmental Changes in Bangong Co Basin (Western Tibet). Part 3: Biogenic Remains. *Palaeogeogr. Palaeoclimatol. Palaeoecol.* 120, 65–78. doi:10.1016/0031-0182(95)00034-8

Fontes, J.-C., Gasse, F., and Gibert, E. (1996). Holocene Environmental Changes in Lake Bangong Basin (Western Tibet). Part 1: Chronology and Stable Isotopes of Carbonates of a Holocene Lacustrine Core. *Palaeogeogr. Palaeoclimatol. Palaeoecol.* 120, 25–47. doi:10.1016/0031-0182(95)00032-1

Gasse, F., Arnold, M., Fontes, J. C., Fort, M., Gibert, E., Huc, A., et al. (1991). A 13,000-year Climate Record from Western Tibet. *Nature* 353, 742–745. doi:10.1038/353742a0

Gasse, F., Fontes, J. C., van Campo, E., and Wei, K. (1996). Holocene Environmental Changes in Bangong Co Basin (Western Tibet). Part 4: Discussion and Conclusions. *Palaeogeogr. Palaeoclimatol. Palaeoecol.* 120, 79–92. doi:10.1016/0031-0182(95)00035-6

Genty, D., Blamart, D., Ghaleb, B., Plagnes, V., Causse, C. H., Bakalowicz, M., et al. (2006). Timing and Dynamics of the Last Deglaciation from European and North African $\delta^{13}C$ Stalagmite Profiles-Comparison with Chinese and South Hemisphere Stalagmites. *Quat. Sci. Rev.* 25 (17), 2118–2142. doi:10.1016/j.quascirev.2006.01.030

Hans Wedepohl, K. (1995). The Composition of the Continental Crust. *Geochimica Cosmochimica Acta* 59, 1217–1232. doi:10.1016/0016-7037(95)00038-2

Holmes, J. A., Allen, M. J., Street-Perrott, F. A., Ivanovich, M., Perrott, R. A., and Waller, M. P. (1999). Late Holocene Palaeolimnology of Bal Lake, Northern Nigeria, a Multidisciplinary Study. *Palaeogeogr. Palaeoclimatol. Palaeoecol.* 148, 169–185. doi:10.1016/s0031-0182(98)00182-5

Holmes, J. A., Street-Peffott, F. A., Ivanovich, M., and Peffott, R. A. (1995). A Late Quaternary Palaeolimnological Record from Jamaica Based on Trace-Element Chemistry of Ostracod Shells. *Chem. Geol.* 124, 143–160. doi:10.1016/0009-2541(95)00032-h

Hou, Y. T., Gou, Y. X., and Chen, D. Q. (2002). *China Ostracodes, Cypridacea and Darwinulidaeceae*, Vol. 1. Beijing: Science Press. (in Chinese).

Hou, Y. T., and Gou, Y. X. (2007). *China Ostracodes, Cytheraceae and Cytherellidae*, Vol. 2. Beijing: Science Press. (in Chinese).

Huang, B. R., Yang, L. F., and Fan, Y. Q. (1985). Ostracodes in Modern Lakes Bottom Sediments of Tibet. *Acta Micropalaeontologica Sin.* 2, 369

Jessen, K. (1938). Some West Baltic Pollen Diagrams. *Quartär* 1, 124

Kasper, T., Frenzel, P., Haberzettl, T., Schwarz, A., Daut, G., Meschner, S., et al. (2013). Interplay between Redox Conditions and Hydrological Changes in Sediments from Lake Nam Co (Tibetan Plateau) during the Past 4000cal BP Inferred from Geochemical and Micropaleontological Analyses. *Palaeogeogr. Palaeoclimatol. Palaeoecol.* 392, 261–271. doi:10.1016/j.palaeo.2013.09.027

Kaufman, A., and Broecker, W. (1965). Comparison of Th230and C14ages for Carbonate Materials from Lakes Lahontan and Bonneville. *J. Geophys. Res.* 70, 4039–4054. doi:10.1029/jz070i016p04039

Kim, B., Cheong, D., and Lee, E. (2015). Paleoenvironmental Changes in Northern Mongolia during the Last Deglaciation Revealed by Trace Element Records in Ostracods from Lake Hovsgol. *Quat. Int.* 384, 169–179. doi:10.1016/j.quaint.2015.04.041

Li, C., Zhou, L., Zhao, Z., Zhang, Z., Zhao, H., Li, X., et al. (2018). In-situ Sr Isotopic Measurement of Scheelite Using fs-LA-MC-ICPMS. *J. Asian Earth Sci.* 160, 38–47. doi:10.1016/j.jseaes.2018.03.025

Li, X., Zhou, X., Liu, W., Wang, Z., He, Y., and Xu, L. (2016). Carbon and Oxygen Isotopic Records from Lake Tuosu over the Last 120 Years in the Qaidam Basin, Northwestern China: The Implications for Paleoenvironmental Reconstruction. *Glob. Planet. Change* 141, 54–62. doi:10.1016/j.gloplacha.2016.04.006

Li, Y. F., Zhang, Q. S., and Li, B. Y. (1994). Ostracod Fauna and Environmental Changes during the Past 17000 Years in the Western Tibet. *Acta Geogr. Sin.* 49 (1), 46

Liu, D., Wang, Y., Cheng, H., Kong, X., and Chen, S. (2013). Centennial-scale Asian Monsoon Variability during the Mid-younger Dryas from Qingtian Cave, Central China. *Quat. Res.* 80, 199–206. doi:10.1016/j.yqres.2013.06.009

Liu, F. X., Liu, D. M., Li, D. W., Zhou, T., and Du, C. C. (2013). Cause and Tectonic Evolution of Bangong Lake Basin. *Earth Sci.-J. Chi. Uni. Geo.* 38 (4), 745. doi:10.3799/dqkx.2013.072

Liu, J. Y., Zheng, M. P., and Wang, H. L. (2007). The Late Part of the Late Pleistocene Microfossil and Environment Change in Zaxi Lake, Middle Tibet. *Acta Geol. Sin.* 81 (12), 1636

Liu, Y., Hu, Z., Gao, S., Günther, D., Xu, J., Gao, C., et al. (2008). *In Situ* analysis of Major and Trace Elements of Anhydrous Minerals by LA-ICP-MS without Applying an Internal Standard. *Chem. Geol.* 257, 34–43. doi:10.1016/j.chemgeo.2008.08.004

Löffler, H. (1997). The Role of Ostracods for Reconstructing Climatic Change in Holocene and Late Pleistocene Lake Environment in Central Europe. *J. Paleolimnol.* 18 (1), 29

Lu, F., An, Z., Chang, H., Dodson, J., Qiang, X., Yan, H., et al. (2017). Climate Change and Tectonic Activity during the Early Pliocene Warm Period from the Ostracod Record at Lake Qinghai, Northeastern Tibetan Plateau. *J. Asian Earth Sci.* 138, 466–476. doi:10.1016/j.jseaes.2017.02.031

Lu, F., An, Z., Dodson, J., Li, X., and Yan, H. (2019). A Late Miocene Ostracod Record from the Northeastern Tibetan Plateau. *J. Paleolimnol.* 61, 297–312. doi:10.1007/s10933-018-0060-x

Ludwig, K. R., and Titterington, D. M. (1994). Calculation of Isochrons, Ages, and Errors. *Geochimica Cosmochimica Acta* 58, 5031–5042. doi:10.1016/0016-7037(94)90229-1

Ma, N., Ma, Z., Zheng, M., and Wang, H. (2012). 230Th Dating of Stem Carbonate Deposits from Tai Cuo Lake, Western Tibetan Plateau, China. *Quat. Int.* 250, 55–62. doi:10.1016/j.quaint.2011.09.012

Ma, Z. B., Ma, N. N., Zhang, X. F., and Wang, Y. (2010a). 230Th/U Chronology of Late Pleistocene Lacustrine Deposits in Zhabuye Salt Lake, Tibetan Plateau. *Acta Geol. Sin.* 84 (11), 1641

Ma, Z. B., Zheng, M. P., Wu, Z. H., and Ma, N. N. (2010b). U-th Isochron Dating of Impure Carbonates and the Possible Effect of Isotopic Fractionation during Leaching. *Acta Geol. Sin.* 84 (8), 1146

Meisch, C. (2000). *Freshwater Ostracoda of Western and Central Europe*. Berlin: Spektrum, 1

IEDQPA and NJGP (1988). *Tertiary Ostracode Fauna from Qaidam Basin, NW China*. Nanjing: Institute of Exploration and Development of Qinghai Petroleum Administration, Nanjing Institute of Geology and Palaeontology of Academia Sinica)Nanjing University Press. (in Chinese).

Peng, H., Ma, Z., Huang, W., and Gao, J. (2014). 230Th/U Chronology of a Paleolithic Site at Xinglong Cave in the Three-Gorge Region of South China. *Quat. Geochronol.* 24, 1–9. doi:10.1016/j.quageo.2014.07.001

Ricketts, R. D., Johnson, T. C., Brown, E. T., Rasmussen, K. A., and Romanovsky, V. V. (2001). The Holocene Paleolimnology of Lake Issyk-Kul, Kyrgyzstan: Trace Element and Stable Isotope Composition of Ostracodes. *Palaeogeogr. Palaeoclimatol. Palaeoecol.* 176, 207–227. doi:10.1016/s0031-0182(01)00339-x

Schwalb, A., Dean, W., Güde, H., Hanisch, S., Sobek, S., and Wessels, M. (2013). Benthic Ostracode δ13C as Sensor for Early Holocene Establishment of Modern Circulation Patterns in Central Europe. *Quat. Sci. Rev.* 66, 112–122. doi:10.1016/j.quascirev.2012.10.032

Schwalb, A. (2003). Lacustrine Ostracodes as Stable Isotope Recorders of Late-Glacial and Holocene Environmental Dynamics and Climate. *J. Paleolimnol.* 29, 267–351. doi:10.1023/a:1024038429005

Schwarcz, H. P., and Latham, A. G. (1989). Dirty Calcites 1. Uranium-Series Dating of Contaminated Calcite Using Leachates Alone. *Chem. Geol. Isot. Geosci. Sect.* 80, 35–43. doi:10.1016/0168-9622(89)90046-8

Shen, Y. P., Liu, G. X., Shi, Y. F., and Zhang, P. Z. (1996). Climate and Environment in the Tibetan Plateau during the Younger Dryas Cooling Event. *J. Glaciol. Geocryol.* 18 (3), 219

Song, G., Wang, H. L., and Zheng, M. P. (2015b). CCA Inferred Environmental Implications of Cammon Ostracods on the Qinghai-Tibetan Plateau. *Acta Geol. Sin. Engl. Ed.* 89 (2), 585

Song, G., Wang, H. L., Zheng, M. P., and Li, J. (2015a). Preliminary Study on Environmental Implications of Ostracodes in Recent Deposits in Tibet. *J. Lake Sci.* 27 (5), 962. doi:10.18307/2015.0524

Tunheng, A., and Hirata, T. (2004). Development of Signal Smoothing Device for Precise Elemental Analysis Using Laser Ablation-ICP-Mass Spectrometry. *J. Anal. At. Spectrom.* 19, 932–934. doi:10.1039/b402493a

Van Campo, E., Cour, P., and Sixuan, H. (1996). Holocene Environmental Changes in Bangong Co Basin (Western Tibet). Part 2: the Pollen Record. *Palaeogeogr. Palaeoclimatol. Palaeoecol.* 120, 49–63. doi:10.1016/0031-0182(95)00033-x

Wang, L., Sun, Z., Cao, H., Li, H.-C., Wang, X., Liu, Y., et al. (2021). A New Method for the U-Th Dating of a Carbonate Chimney Deposited during the Last Glaciation in the Northern Okinawa Trough, East China Sea. *Quat. Geochronol.* 66, 101199. doi:10.1016/j.quageo.2021.101199

Williams, D. F., Kuzmin, M. I., Prokopenko, A. A., Karabanov, E. B., Khursevich, G. K., and Bezrukova, E. V. (2001). The Lake Baikal Drilling Project in the Context of a Global Lake Drilling Initiative. *Quat. Int.* 80-81, 3–18. doi:10.1016/s1040-6182(01)00015-5

Yang, F., Qiao, Z. Z., Zhang, H. Q., Zhang, Y. H., and Sun, Z. C. (2006). Features of the Cenozoic Ostracod Fauna and Environmental Significance in Qaidam Basin. *J. Palaeogeogr.* 8, 143. doi:10.3969/j.issn.1671-1505.2006.02.001

Yang, Q., Jochum, K. P., Stoll, B., Weis, U., Börner, N., Schwalb, A., et al. (2014). Trace Element Variability in Single Ostracod Valves as a Proxy for Hydrochemical Change in Nam Co, Central Tibet, During the Holocene. *Palaeogeogr. Palaeoclimatol. Palaeoecol.* 399, 225–235. doi:10.1016/j.palaeo.2014.01.014

Yang, Y., Fang, X., Appel, E., Galy, A., Li, M., and Zhang, W. (2013). Late Pliocene-Quaternary Evolution of Redox Conditions in the Western Qaidam Paleolake (NE Tibetan Plateau) Deduced from Mn Geochemistry in the Drilling Core SG-1. *Quat. Res.* 80, 586–595. doi:10.1016/j.yqres.2013.07.007

Yilmaz, F., and Külköylüoglu, O. (2006). Tolerance, Optimum Ranges, and Ecological Requirements of Freshwater Ostracoda (Crustacea) in Lake Aladag (Bolu Turkey). *Ecol. Res.* 21 (2), 16. doi:10.1007/s11284-005-0121-2

Zhao, J., An, C.-B., Huang, Y., ChenMorrill, F.-H., and Chen, F., H. (2017). Contrasting Early Holocene Temperature Variations between Monsoonal East Asia and Westerly Dominated Central Asia. *Quat. Sci. Rev.* 178, 14–23. doi:10.1016/j.quascirev.2017.10.036

Zheng, M. P., Liu, J. Y., Pang, Q. Q., Ma, Z. B., Wang, H. L., and Ma, N. N. (2012). Sedimentary Records and the Late Pleistocene-Holocene Climatic Changes in Tai Co, Tibet (Xizang). *Acta Geol. Sin.* 86 (1), 104.

Conflict of Interest: The authors declare that the research was conducted in the absence of any commercial or financial relationships that could be construed as a potential conflict of interest.